

# Antihyperon potentials in nuclei via exclusive antiproton-nucleus reactions at FAIR

Alicia Sanchez Lorente<sup>a</sup>, Sebastian Bleser<sup>a</sup>, Sebastian Bleser<sup>a</sup>, Josef Pochodzalla<sup>a,b,\*</sup>

<sup>a</sup>*Helmholtz Institute Mainz, Johannes Gutenberg-Universität Mainz, D-55099 Mainz, Germany*

<sup>b</sup>*Institut für Kernphysik, Johannes Gutenberg-Universität Mainz, D-55099 Mainz, Germany*

## Abstract

The exclusive production of hyperon-antihyperon pairs close to their production threshold in  $\bar{p}$  - nucleus collisions offers a unique and hitherto unexplored opportunity to elucidate the behaviour of antihyperons in nuclei. For the first time we analyse these reactions in a microscopic transport model using the the Gießen Boltzmann-Uehling-Uhlenbeck transport model. The calculation take the delicate interplay between the strong absorption of antihyperons, their rescattering and refraction at the nuclear surface as well as the Fermi motion of the struck nucleon into account. We find a substantial sensitivity of transverse momentum correlations of coincident  $\bar{\Lambda}\Lambda$ -pairs to the assumed depth of the  $\bar{\Lambda}$ -potential. Because of the high cross section for this process and the simplicity of the experimental method our results are highly relevant for future activities at the international Facility for Antiproton and Ion Research (FAIR).

*Keywords:*

Antiproton nucleus reaction, Antihyperon production

PACS: 25.43.+t, 14.20.Jn, 5.80.Pw

## 1. Introduction

The interaction of individual baryons or antibaryons in nuclei provides a unique opportunity to elucidate strong in-medium effects in baryonic systems. While for neutrons and protons as well as some strange baryons experimental information on their binding in nuclei exists, information on antibaryons in nuclei are rather scarce. Only for the antiproton the nuclear potential could be constrained by experimental studies. The (Schrödinger equivalent) antiproton potential at normal nuclear density turns out to be in the range of  $U_{\bar{p}} \approx -150\text{MeV}$ , i.e. a factor of approximately 4 weaker than expected from naive G-parity relations [1]. Gaitanos *et al.* [2] suggested that this discrepancy can be traced back to the missing energy dependence of the proton-nucleus optical potential in conventional relativistic mean-field models. The required energy and momentum dependence could be recovered by extending the relativistic hadrodynamics Lagrangian by non-linear derivative interactions [3, 2, 4] thus also mimicking many-body forces [5]. Considering the important role played e.g. by strange baryons and antibaryons production for a quantitative interpretation of high-energy heavy-ion collisions and dense hadronic systems it is clearly mandatory to test these concepts also in the strangeness sector. Furthermore, it was pointed out recently [6] that in-medium interactions of antibaryons may cause compressional effects and may thus provide additional information on the nuclear equation-of-state [7]. Therefore, the question if and to what extend G-parity is violated by antihyperons in nuclei is also a challenging problem by itself.

Antihyperons annihilate quickly in nuclei and conventional spectroscopic studies of bound systems comparable to hypernuclei are not feasible. As a consequence, no experimental information on the nuclear potential of antihyperons exists so far. As suggested recently [8], quantitative information on the antihyperon potentials may be obtained via exclusive antihyperon-hyperon pair production close to threshold in antiproton-nucleus interactions. Once these hyperons and antihyperons leave the nuclear environment they can be detected and their asymptotic momentum distributions will reflect the depth of the respective potentials. In ref. [8] it was demonstrated that momentum correlations of emitted hyperon-antihyperon pairs can be used to extract information on the relative potential of hyperons and antihyperons in nuclei. Since in the  $\bar{p}p$  center-of-mass the distribution of the free baryon-antibaryon pairs is non-isotropic, the analysis relied mainly on the *transverse* momenta of the coincident baryons and antibaryons. The calculations of Ref. [8] revealed significant sensitivities of the transverse momentum asymmetry  $\alpha_T$  which is defined in terms of the transverse momenta of the coincident particles

$$\alpha_T = \frac{p_T(\Lambda) - p_T(\bar{\Lambda})}{p_T(\Lambda) + p_T(\bar{\Lambda})}. \quad (1)$$

to the depth of the antihyperon potential. The asymmetry  $\alpha_T$  turned out to be rather robust in case of model parameter variations and remained substantial also if the momentum dependence of the potential was considered [9]. However, these schematic simulations ignored rescattering processes and refractive effects at the potential boundary. These effects are expected to erode the two-body character of the  $\bar{\Lambda}\Lambda$  production and may thus diminish or even destroy the sensitivity. In order to go be-

\*Corresponding author

Email address: pochodza@kph.uni-mainz.de (Josef Pochodzalla)

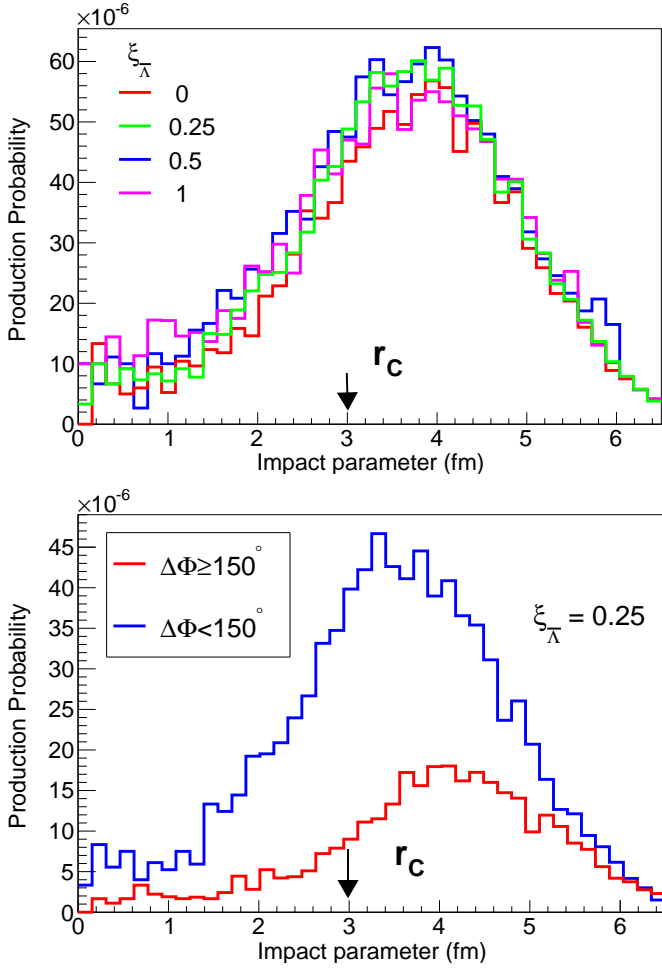


Figure 1: Top: Probability distribution for free  $\Lambda\bar{\Lambda}$ -pair production in 0.85 GeV  $\bar{p}+^{20}\text{Ne}$  collisions as a function of the impact parameter. The different lines show the GiBUU predictions for different scaling factor  $\xi_{\bar{\Lambda}}$  of the  $\Lambda$ -potentials. Bottom: Impact parameter distributions for planar ( $\Delta\Phi \geq 150^\circ$ ) and non-planar ( $\Delta\Phi < 150^\circ$ )  $\Lambda\bar{\Lambda}$  pairs (cf. Fig. 2) using a fixed  $\bar{\Lambda}$ -potential scaling factor  $\xi_{\bar{\Lambda}} = 0.25$ . The arrows mark the rms-charge radius  $r_c$  of  $^{20}\text{Ne}$

yond the schematic calculations presented in Refs. [8, 9] and to include simultaneously rescattering, refraction and absorption effects, we present here first realistic calculations of this new observable with a microscopic transport model.

## 2. Transport calculations of antihyperon-hyperon production

The Giessen Boltzmann-Uehling-Uhlenbeck transport model (GiBUU, Release 1.5) [10] describes many features of  $\bar{p}$ -nucleus interactions in the FAIR energy range [1, 10, 11]. Particularly the presently available data on strangeness production are well reproduced. In this code non-linear derivative interactions [2] are not yet included and a simple scaling factor  $\xi_{\bar{p}} = 0.22$  is applied to ensure a Schrödinger equivalent antiproton potential of  $-150\text{ MeV}$  at saturation density [11]. (Note that this value differs slightly from the scaling factor  $\xi_{\bar{p}} = 0.25$  given in Ref. [1].) The hyperon potentials were fixed by hypernuclear and hyperatom data [11]. No experimental informa-

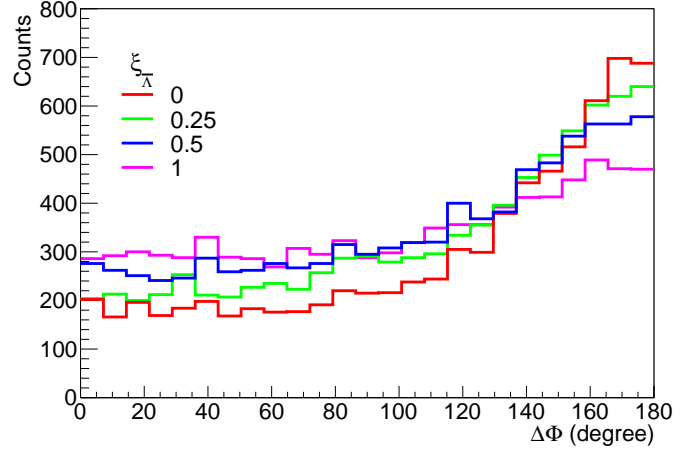


Figure 2: Coplanarity of coincident  $\Lambda\bar{\Lambda}$ -pairs produced exclusively in 0.85 GeV  $\bar{p}+^{20}\text{Ne}$  interactions. The different histograms show the GiBUU predictions for different scaling factor  $\xi_{\bar{\Lambda}}$  of the  $\Lambda$ -potentials.

tion exists for antihyperons in nuclei and G-parity symmetry is therefore used to specify their default potentials. This leads to a  $\bar{\Lambda}$ -potential  $U(\bar{\Lambda}) = -449\text{ MeV}$ . As already stressed in ref. [11], the attractive  $\Sigma$ -potential and the weak attraction for kaons adopted in the GiBUU model is not compatible with experimental data. In the present work we focus on exclusive  $\Lambda\bar{\Lambda}$ -pair production in the threshold region. Therefore, we do not expect that a more realistic treatment of the  $\Sigma$  and kaon potentials will modify the conclusions of the present study.

We have studied the exclusive reaction  $\bar{p}+^{20}\text{Ne} \rightarrow \bar{\Lambda}\Lambda$  at beam energies of 0.85 GeV and 1 GeV. These energies correspond to antiproton momenta of 1.522 GeV/c and 1.696 GeV/c, respectively. At 0.85 GeV the excess energy with respect to the elementary reaction  $\bar{p}+p \rightarrow \bar{\Lambda}\Lambda$  amounts to only 30.6 MeV. Therefore, the  $\bar{\Sigma}\Lambda$  and  $\Sigma\bar{\Lambda}$  channels are not accessible and also the production of a pion in addition to a  $\Lambda\bar{\Lambda}$ -pair can be neglected. The higher energy of 1 GeV lies above the  $\bar{\Sigma}\Lambda$ -threshold and makes also the  $\bar{p}n \rightarrow \bar{\Lambda}\Sigma^-$  and  $\bar{p}p \rightarrow \bar{\Lambda}\Sigma^0$  as well as their charge conjugate channels accessible. Those channels will be discussed in a forthcoming paper.

In order to explore the sensitivity of the transverse momentum asymmetry on the depth of the  $\bar{\Lambda}$ -potential we have performed a series of calculations where only the antihyperon potentials were modified by a single scaling factor  $\xi_{\bar{\Lambda}}$ , leaving all other input parameters of the model unchanged. The calculations were performed at the High Power Computing Cluster HIMSTER located at the Helmholtz-Institute Mainz. Each GiBUU-Job comprised 1000 parallel events. In order to keep the necessary computing time low, all cross sections for antihyperon – hyperon pair production were artificially enhanced by a factor of 10. Since within the 1000 parallel events of an individual job the probability of a multiple production of hyperon pairs is low, the mean field dynamics is insignificantly distorted. For each parameter set a total of 26460 Jobs were generated. Each parameter set shown in the following contains approximately 8000  $\bar{\Lambda}\Lambda$ -pairs where both, the  $\bar{\Lambda}$  and the  $\Lambda$  escaped the nucleus.

Unlike in inclusive reactions [12, 13], the strong absorption of the antihyperons in nuclei favors the production of free hyperon-antihyperon pairs in the corona of the target nucleus. Configurations where the path of the antihyperon within the target nucleus is minimal or where secondary scattering reduces this path length towards the nuclear surface will be more likely to produce free  $\bar{\Lambda}\Lambda$ -pairs. The top part of Fig. 1 shows the probability for free  $\bar{\Lambda}\Lambda$ -pair production ( $\sim b^{-1}dN_{\bar{\Lambda}\Lambda}/db$ ) as a function of the impact parameter  $b$  for different  $\bar{\Lambda}$ -potentials. (The artificial increase for antihyperon-hyperon production by a factor of 10 is taken into account.) The distributions peak around 3.8 fm which is significantly larger than the  $^{20}\text{Ne}$  rms-charge radius of  $r_C = 3.0$  fm [14] marked by the arrow in Fig. 1. Consequently, free antihyperon-hyperon pairs are mainly produced at low nuclear densities corresponding to 20 to 25% of the central density.

### 3. Results and discussion

For scaling factors  $\xi_{\bar{\Lambda}}$  between 1 and 0.25 the average impact parameter persists at 3.8 fm. Only for  $\xi_{\bar{\Lambda}}=0$  a slight increase to 3.9 fm is observed. At the same time the number of produced  $\bar{\Lambda}\Lambda$ -pairs remains fairly constant on a level of about 8700 events over the range  $1 \leq \xi_{\bar{\Lambda}} \leq 0.5$  and decreases for  $\xi_{\bar{\Lambda}} = 0$  by about 15% to  $\approx 7500$  events. This moderate decrease indicates that absorption does not change dramatically with the depth of the  $\bar{\Lambda}$ -potential. In Fig. 1 (top) the main variations are seen at small impact parameter. This suggests that the smaller number of events in case of a shallow antihyperon potential is caused by an increased absorption at more central collisions. For a quantitative interpretation one has to keep in mind, however, that also a potential-dependent rescattering can enhance the escape probability from the nucleus by decreasing the path length until the nuclear surface of particularly the antihyperons.

The role of secondary deflection can be explored by the coplanarity of the  $\bar{\Lambda}\Lambda$ -pairs. (Of course, in these reactions close to threshold the Fermi motion of the struck proton inside the nuclear target contributes also to the final momenta.) Fig. 2 shows the angle  $\Delta\Phi$  defined as the difference between the azimuthal angles of the free  $\bar{\Lambda}$  and  $\Lambda$ . Already for zero  $\bar{\Lambda}$ -potential, the coplanarity is strongly blurred. With increasing potential depth for the  $\bar{\Lambda}$ , the coplanarity is even less pronounced. The significant deviation from  $180^\circ$  demonstrates the influence of secondary scattering prior to the emission of the  $\bar{\Lambda}$  or  $\Lambda$  or a deflection at the potential boundary.

The effect of enhanced secondary scattering processes in the case of deep antihyperon potentials is also visible in the momentum distributions of the emitted particles. Elastic scattering will on the average decrease the longitudinal momentum and will broaden the transverse momentum distribution. Fig. 3 shows the longitudinal momenta (top) and transverse momenta (bottom) for  $\bar{\Lambda}$  and  $\Lambda$ -hyperons from exclusive pair production. Since the antihyperons are emitted more forward in the center of mass, their (longitudinal) momentum distributions peak at values around  $0.9 \text{ GeV}/c$ , while for  $\Lambda$ -hyperons the typical momenta reach only half of this value. The decrease of the longitudinal momenta for both,  $\Lambda$ -hyperons as well as  $\bar{\Lambda}$ -hyperons

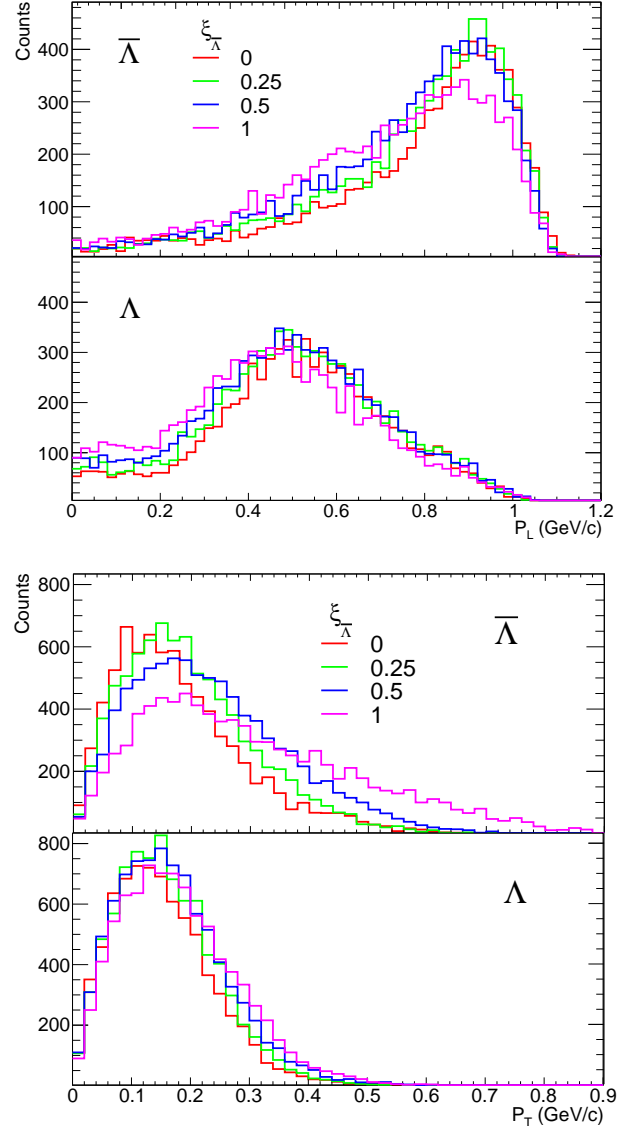


Figure 3: Longitudinal (top) and transverse momentum distributions (bottom) for  $\Lambda$  and  $\bar{\Lambda}$  from exclusive pair production. The different symbols show the GiBUU predictions for different scaling factors  $\xi_{\bar{\Lambda}}$  of the  $\bar{\Lambda}$ -potential.

with deeper antihyperon potentials and hence more rescattering (c.f. Fig. 2) is clearly seen in the top part of Fig. 3. Because of the larger initial longitudinal momenta, scattering in the target nucleus is expected to lead to a larger absolute broadening of the  $\bar{\Lambda}$  transverse momentum distributions as compared to the lower momentum  $\Lambda$ -hyperons. As can be seen in the lower part of Fig. 3, the increase of the transverse momenta with deeper  $\bar{\Lambda}$ -potential is indeed more pronounced for  $\bar{\Lambda}$ -hyperons than for  $\Lambda$ -hyperons.

The delicate interplay between the Fermi motion of the struck nucleon, the absorption, rescattering and refraction at the nuclear surface of the produced hyperons and antihyperons is further illustrated in the bottom part of Fig. 1. Coplanar  $\bar{\Lambda}\Lambda$ -pairs with  $\Delta\Phi \geq 150^\circ$  are associated with larger impact parameters ( $\langle b \rangle_{\Delta\Phi \geq 150^\circ} = 4.1 \text{ fm}$ ) as compared to the case  $\Delta\Phi < 150^\circ$  where

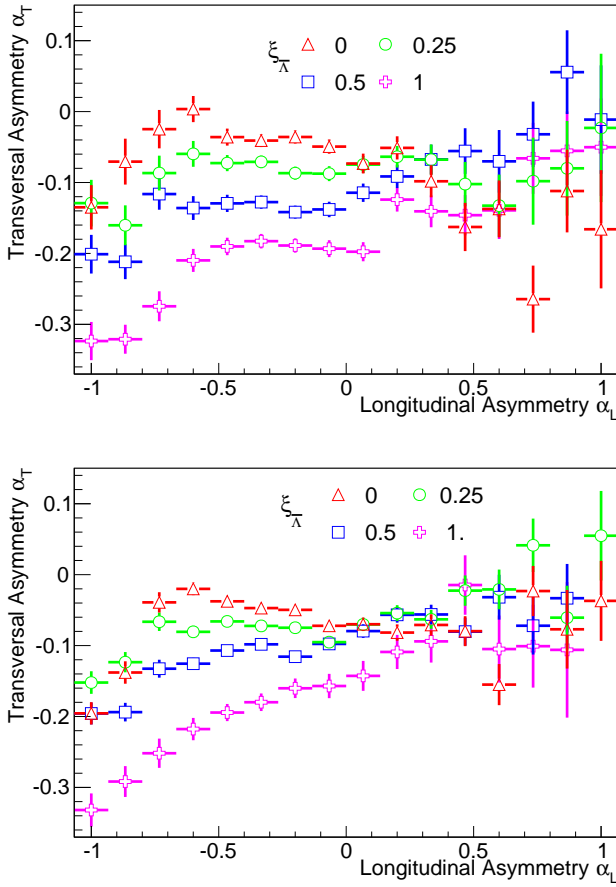


Figure 4: Average transverse momentum asymmetry  $\alpha_T$  (Eq. 1) as a function of the longitudinal momentum asymmetry for  $\Lambda\bar{\Lambda}$ -pairs produced exclusively in 0.85 GeV (top) and 1 GeV (bottom)  $\bar{p}+^{20}\text{Ne}$  interactions. The different symbols show the GiBUU predictions for different scaling factor  $\xi_{\bar{\Lambda}}$  of the  $\bar{\Lambda}$ -potentials.

scattering processes contribute more ( $\langle b \rangle_{\Delta\Phi < 150^\circ} = 3.7$  fm). The figure suggests that at small impact parameters the rescattering is indeed crucial for antihyperons being able to escape from the nucleus.

In Fig. 4 we finally show the GiBUU prediction for the transverse asymmetry  $\alpha_T$  (Eq. 1) for different scaling factors  $\xi_{\bar{\Lambda}}$  of the  $\bar{\Lambda}$ -potential. As in Ref. [8] we plot the average  $\alpha_T$  as a function of the longitudinal momentum asymmetry  $\alpha_L$  which is defined for each event as

$$\alpha_L = \frac{p_L(\Lambda) - p_L(\bar{\Lambda})}{p_L(\Lambda) + p_L(\bar{\Lambda})}. \quad (2)$$

For 0.85 GeV (top) as well as 1 GeV (bottom) antiproton energy a remarkable sensitivity of  $\alpha_T$  on the  $\bar{\Lambda}$ -potential is found at negative values of  $\alpha_L$ . Despite the concern mentioned in the introduction, secondary effects do not wipe out the dependence of  $\alpha_T$  on the antihyperon potential. Both, this significant larger sensitivity as compared to the schematic calculation in Ref. [8] as well as the shift of the average  $\alpha_T$  towards more negative values are linked to the substantial transverse momentum broadening for the  $\bar{\Lambda}$ -hyperons by secondary scattering (c.f. lower part of Fig. 3). For positive values of  $\alpha_L$  where the antihyperon is

emitted backward with respect to  $\Lambda$ -particle, the statistics in the present simulation is too low to draw quantitative conclusions. But even in this region of  $\alpha_L$  a systematic variation of  $\alpha_T$  with the antihyperon potential might show up with improved statistics.

The international Facility for Antiproton and Ion Research (FAIR) presently under construction in Darmstadt (Germany) will provide high intensity antiproton beams with momenta between 1.5 GeV/c and 15 GeV/c. A unique feature of antiproton interactions in the energy range of PANDA is the large production cross section of hyperon-antihyperon pairs [15]. At its full luminosity the production rate of  $\bar{Y}Y$ -pairs range from a few 100 per second for the  $\bar{\Xi}\Xi$ -channel, up to a few thousand per second for the  $\bar{\Lambda}\Lambda$ -channel in the elementary  $\bar{p}p$ -reaction. Due to the strong absorption of antibaryons in nuclei this production rate will be lowered depending on the size of the target nucleus in antiproton-nucleus collisions. According to the GiBUU calculations presented above, for a typical medium size target nucleus like  $^{20}\text{Ne}$  still several hundreds free  $\bar{\Lambda}\Lambda$ -pairs can be produced per second. For a nuclear target in this mass range and at maximum interaction rate, approximately 10 reconstructed  $\bar{\Lambda}\Lambda$ -pairs per second are expected [16]. Therefore, a measurement period of about one hour will provide a statistics exceeding that of the GiBUU simulations shown above. This will be sufficient to reach a precision of about 10% for the scaling factor  $\xi_{\bar{\Lambda}}$  of the antilambda potential. These numbers illustrate that even on rather pessimistic assumption about the luminosity and/or the availability of the antiproton beam during the commissioning phase of the PANDA experiment, one can reach unique and relevant information on the behavior of strange antibaryons in nuclei shortly after the delivery of the first antiproton beam at FAIR.

This work was supported in part by European Community Research Infrastructure Integrating Activity 'Study of Strongly Interacting Matter' HadronPhysics3 (SPHERE) under the FP7.

## References

- [1] A.B. Larionov, I.A. Pshenichnov, I.N. Mishustin, and W. Greiner, Phys. Rev. C 80 (2009) 021601(R).
- [2] T. Gaitanos, M. Kaskulov, H. Lenske, Phys. Lett. B 703 (2011) 193.
- [3] T. Gaitanos, M. Kaskulov, U. Mosel, Nucl. Phys. A 828 (2009) 9.
- [4] T. Gaitanos, M. Kaskulov, Nucl. Phys. A 899 (2013) 133.
- [5] R.O. Gomes, V.A. Dexheimer, S. Schramm, C.A.Z. Vaconcellos, arXiv:1411.4875 [astro-ph.SR].
- [6] A.B. Larionov, I.N. Mishustin, L.M. Satarov, W. Greiner, Phys. Rev. C 82 (2010) 024602.
- [7] T. Gaitanos and M. Kaskulov, arXiv:1503.00625v1 [nucl-th].
- [8] J. Pochodzalla, Phys. Lett. B 669 (2008) 306.
- [9] J. Pochodzalla, Hyperfine Interact. 194 (2009) 255.
- [10] O. Buss *et al.*, Phys. Rep. 512 (2012) 1.
- [11] A.B. Larionov, T. Gaitanos, and U. Mosel, Phys. Rev. C 85 (2012) 024614.
- [12] A. Sibirtsev, K. Tsushima, and A.W. Thomas, Eur. Phys. J. A 6 (1999) 351.
- [13] H. Lenske and P. Kienle, Phys. Lett. B 647 (2007) 82.
- [14] H. De Vries, C.W. De Jager, and C. De Vries, At. Data and Nucl. Data Tables 36 (1987) 495.
- [15] Physics Performance Report for PANDA: Strong Interaction Studies with Antiprotons, arXiv:0903.3905 [hep-ex].
- [16] PANDA Collaboration, Technical Progress Report (GSI Darmstadt), pp. 1-383 (2005).